11-17-2008

Comparison of post-newtonian and numerical evolutions of black-hole binaries

Hiroyuki Nakano
Rochester Institute of Technology

Manuela Campanelli
Rochester Institute of Technology

Carlos Lousto
Rochester Institute of Technology

Yosef Zlochower
Rochester Institute of Technology

Comparison of Post-Newtonian and Numerical Evolutions of Black-Hole Binaries

Hiroyuki Nakano[1], Manuela Campanelli[2], Carlos O. Lousto[3], and Yosef Zlochower[4]

Center for Computational Relativity and Gravitation, and School of Mathematical Sciences, Rochester Institute of Technology, Rochester, New York 14623, USA

Abstract

In this paper, we compare the waveforms from the post-Newtonian (PN) approach with the numerical simulations of generic black-hole binaries which have mass ratio $q \sim 0.8$, arbitrarily oriented spins with magnitudes $S_1/m_1^2 \sim 0.6$ and $S_2/m_2^2 \sim 0.4$, and orbit 9 times from an initial orbital separation of $r \approx 11M$ prior to merger. We observe a reasonably good agreement between the PN and numerical waveforms, with an overlap of over 98% for the first six cycles of the $(\ell = 2, m = \pm 2)$ mode and over 90% for the $(\ell = 2, m = 1)$ and $(\ell = 3, m = 3)$ modes.

1 Introduction

In 2005, two complementary and independent methods were discovered that allowed numerical relativists to completely solve the black-hole binary problem in full strong-field gravity [1, 2, 3]. On the other hand, there are currently major experimental and theoretical efforts underway to measure these gravitational wave signals. Therefore, one of the most important tasks of numerical relativity (NR) is to assist gravitational wave observatories in detecting gravitational waves and extracting the physical parameters of the sources. Given the demanding resources required to generate these black-hole binary simulations, it is necessary to develop various techniques in order to model arbitrary binary configuration based on numerical simulations in combination with post-Newtonian (PN) and perturbative (e.g. black-hole perturbation) calculations.

In this paper, we compare the NR and PN waveforms for the challenging problem of a generic black-hole binary, i.e., a binary with unequal masses and unequal, non-aligned, and precessing spins. Comparisons of numerical simulations with post-Newtonian ones have several benefits aside from the theoretical verification of PN. From a practical point of view, one can directly propose a phenomenological description and thus make predictions in regions of the parameter space still not explored by numerical simulations. From the theoretical point of view, an important application is to have a calibration of the post-Newtonian error in the last stages of the binary merger.

The paper is organized as follows. In Sec. II we present our method to derive the PN gravitational waveforms from generic black-hole binaries, and in III we compare the NR and PN waveforms. Finally in Sec. IV we summarize this paper and discuss remaining problems. The detailed numerical method and PN calculation presented here have been given in [4].

2 Gravitational waveforms in the PN approach

In order to calculate PN gravitational waveforms, we need to calculate the orbital motion of binaries in the post-Newtonian approach. Here we use the ADM-TT gauge, which is the closest to our quasi-isotropic numerical initial data coordinates. In this paper, we use the PN equations of motion (EOM) based on [5, 6, 7]. The Hamiltonian is given in [5], with the additional terms, i.e., the next-to-leading

[1]E-mail:hxnsma@rit.edu
[2]E-mail:manuela@astro.rit.edu
[3]E-mail:colsma@rit.edu
[4]E-mail:yrzsma@rit.edu

order gravitational spin-orbit and spin-spin couplings provided in [6, 7], and the radiation-reaction force given in [5]. The Hamiltonian which we used here is given by

$$\begin{aligned} H &= H_{\rm O,Newt} + H_{\rm O,1PN} + H_{\rm O,2PN} + H_{\rm O,3PN} \\ &\quad + H_{\rm SO,1.5PN} + H_{\rm SO,2.5PN} + H_{\rm SS,2PN} + H_{\rm S_1S_2,3PN}\,, \end{aligned} \tag{1}$$

where the subscript O, SO and SS denote the pure orbital (non-spinning) part, spin-orbit coupling and spin-spin coupling, respectively, and Newt, 1PN, 1.5PN, etc., refer to the perturbative order in the post-Newtonian approach. From this Hamiltonian, the conservative part of the orbital and spin EOM is derived using the standard techniques of the Hamiltonian formulation. For the dissipative part, we use the non-spinning radiation reaction results up to 3.5PN (which contributes to the orbital EOM at 6PN order), as well as the leading spin-orbit and spin-spin coupling to the radiation reaction [5].

The above PN evolution is used both to produce very low eccentricity orbital parameters at $r \approx 11M$ from an initial orbital separation of $50M$, and to evolve the orbit from $r \approx 11M$. We use these same parameters at $r \approx 11M$ to generate the initial data for our numerical simulations. The initial binary configuration at $r = 50M$ had the mass ratio $q = m_1/m_2 = 0.8$, $\vec{S}_1/m_1^2 = (-0.2, -0.14, 0.32)$, and $\vec{S}_2/m_2^2 = (-0.09, 0.48, 0.35)$.

We then construct a hybrid waveform from the orbital motion by using the following procedure. First we use the 1PN accurate waveforms derived by Wagoner and Will [8] (WW waveforms) for a generic orbit. By using these waveforms, we can introduce effects due to the black-hole spins, including the precession of the orbital plane. On the other hand, Blanchet *et al.* [9] recently obtained the 3PN waveforms (B waveforms) for non-spinning circular orbits. We combine these two waveforms to produce a hybrid waveform. In order to combine the WW and B waveforms, we need to take into account differences in the definitions of polarization states and the angular coordinates. The WW waveforms use the standard definition of GW polarization states, which are the same as those derived from the Weyl scalar, but the B waveforms use an alternate definition. The angular coordinates in the B waveforms are derived from circular orbits in the equatorial (xy) plane. To directly compare the NR and PN waveforms, we must add a time dependent inclination to the B waveforms because in the generic case the orbital planes are inclined with respect to the xy plane.

We note that since there is no gauge ambiguity for combining the two waveforms, the combination of the WW and B waveforms is unique. Also, it should be noted that we calculate the spin contribution to the waveforms through its effect on the orbital motion directly in the WW waveforms and indirectly in B waveforms through the inclination of the orbital plane.

For the NR simulations we calculate the Weyl scalar ψ_4 and then convert the (ℓ, m) modes of ψ_4 into (ℓ, m) modes of $h = h_+ - ih_\times$.

3 Comparison of the NR and PN waveforms

To compare PN and numerical waveforms, we need to determine the time translation δt between the numerical time and the corresponding point on the PN trajectory. That is to say, the time it takes for the signal to reach the extraction sphere ($r = 100M$ in our numerical simulation). We determine this by finding the time translation near $\delta t = 100M$ that maximizes the agreement of the early time waveforms in the $(\ell = 2, m = \pm 2)$, $(\ell = 2, m = \pm 1)$, and $(\ell = 3, m = \pm 3)$ simultaneously. We find $\delta t \sim 112$, in good agreement with the expectation for our observer at $r = 100M$. Since our PN waveforms are given uniquely by a binary configuration, i.e., an actual location of the PN particle, we do not have any time shift or phase modification other than this retardation of the signal. It is noted that other methods which are not based on the particle locations, have freedom in choosing a phase factor.

In the left panel of Fig. 1, we show the real part of the $(\ell = 2, m = 2)$ mode of the strain h with this time translation. (The other modes are shown in [4].) We note that the reasonable agreement of the numerical and PN waveforms for $700M$.

From the analysis of the amplitudes of each mode, we see that the precession and eccentricity of the orbit impart signatures on the modes of the waveform at the orbital frequency. However, the long-time oscillations in the amplitudes, here apparent only in the ($\ell = 2$, $m = \pm 1$) modes, seem to be due purely to

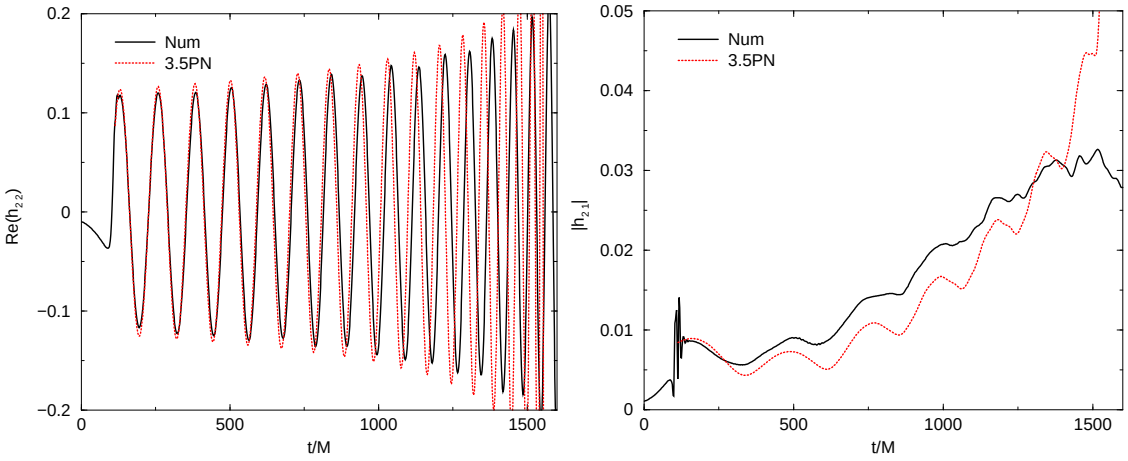

Figure 1: **Left:** The real part of the $(\ell = 2, m = 2)$ mode of h from the numerical and 3.5PN simulations. Here 3.5PN predicts an early merger and has a higher frequency than the numerical waveform. **Right:** The amplitude of the $(\ell = 2, m = 1)$ mode of h from the numerical and 3.5PN simulations. The secular oscillation in the numerical amplitude occurs at roughly the precessional frequency. The timescale is of order $1000M$. Here the shorter-timescale oscillations correspond roughly to the orbital period.

precession, and occur at the precessional frequency. In the right panel of Fig. 1, we show the amplitudes of the $(\ell = 2, m = 1)$ mode of h.

Next, in order to quantitatively compare the modes of the PN waveforms with the numerical waveforms we define the overlap, or matching criterion, for the real and imaginary parts of each mode as

$$M^{\Re}_{\ell m} = \frac{< R^{\rm Num}_{\ell m}, R^{\rm PN}_{\ell m} >}{\sqrt{< R^{\rm Num}_{\ell m}, R^{\rm Num}_{\ell m} >< R^{\rm PN}_{\ell m}, R^{\rm PN}_{\ell m} >}}\,, \quad M^{\Im}_{\ell m} = \frac{< I^{\rm Num}_{\ell m}, I^{\rm PN}_{\ell m} >}{\sqrt{< I^{\rm Num}_{\ell m}, I^{\rm Num}_{\ell m} >< I^{\rm PN}_{\ell m}, I^{\rm PN}_{\ell m} >}}\,, \tag{2}$$

where $R_{\ell m}$ and $I_{\ell m}$ are defined by the real and imaginary parts of the waveform mode $h_{\ell m}$, respectively, and the inner product is calculated by $< f, g >= \int_{t_1}^{t_2} f(t)g(t)dt$. Hence, $M^{\Re}_{\ell m} = M^{\Im}_{\ell m} = 1$ indicates that the given PN and numerical mode agree. The results of these matching studies are summarized in Table 1.

Table 1: The match of the real and imaginary parts of the modes of h of the G3.5 configuration for the 3.5 PN waveforms and the numerical waveforms with the time translation $\delta t = 112.5$.

Integration Time	600	800	1000
$M^{\Re}_{22}$	0.986	0.964	0.895
$M^{\Im}_{22}$	0.987	0.962	0.900
$M^{\Re}_{2-2}$	0.986	0.964	0.895
$M^{\Im}_{2-2}$	0.987	0.962	0.901
$M^{\Re}_{21}$	0.904	0.912	0.843
$M^{\Im}_{21}$	0.916	0.901	0.820
$M^{\Re}_{2-1}$	0.920	0.908	0.833
$M^{\Im}_{2-1}$	0.917	0.903	0.816
$M^{\Re}_{33}$	0.938	0.891	0.738
$M^{\Im}_{33}$	0.919	0.868	0.721
$M^{\Re}_{3-3}$	0.931	0.880	0.733
$M^{\Im}_{3-3}$	0.906	0.857	0.721

We also determine an alternate time translation, one wavelength in the $(\ell = 2, m = 2)$ mode, that increases the matching of the $(\ell = 2, m = 2)$ mode over longer integration periods. On the other hand, this new time translation, $\delta t = 233$, causes the $(\ell = 3)$ modes to be out of phase, leading to negative overlaps. Thus by looking at the $(\ell = 2)$ and $(\ell = 3)$ modes simultaneously, we can reject this false match.

4 Conclusion and discussion

We analyzed the first long-term generic waveform produced by the merger of unequal mass, unequal spins, precessing black holes. It is found that a good initial agreement of waveforms for the first six cycles, with overlaps of over 98% for the $(\ell = 2, m = \pm 2)$ modes, over 90% for the $(\ell = 2, m = \pm 1)$ modes, and over 90% for the $(\ell = 3, m = \pm 3)$ modes. These agreement degrades as we approach the more dynamical region of the late merger and plunge.

There are some remaining problems. The PN gravitational waveforms used here do not include direct spin effects. We considered the spin contribution to the waveform only through its effect on the orbital motion. Recently, the direct spin effects have been discussed in [10]. And also in the PN approach, the waveforms are derived from binaries whose each body is considered as a point particle. The finite size effects of the bodies is also important in the late-inspiral region. Furthermore, we will need higher-order post-Newtonian calculations of both spin-orbit and spin-spin terms, especially for the phase evolution of gravitational waves.

We also have a important issue. In order to detect the gravitational waves from binaries, it is necessary to study the data analysis. (For example, the Numerical INJection Analysis (NINJA) project [11].) Here, we must treat a very large parameter space for intrinsic parameters of black-hole binaries, The development of effective GW templates for the whole history of binaries, i.e., the inspiral, merger and ringdown should be done.

Acknowledgments

We would like to thank H. Tagoshi and R. Fujita for useful discussions.

References

[1] F. Pretorius, Phys. Rev. Lett. **95**, 121101 (2005) [arXiv:gr-qc/0507014].

[2] M. Campanelli, C. O. Lousto, P. Marronetti and Y. Zlochower, Phys. Rev. Lett. **96**, 111101 (2006) [arXiv:gr-qc/0511048].

[3] J. G. Baker, J. Centrella, D. I. Choi, M. Koppitz and J. van Meter, Phys. Rev. Lett. **96**, 111102 (2006) [arXiv:gr-qc/0511103].

[4] M. Campanelli, C. O. Lousto, H. Nakano and Y. Zlochower, arXiv:0808.0713 [gr-qc].

[5] A. Buonanno, Y. Chen and T. Damour, Phys. Rev. D **74**, 104005 (2006) [arXiv:gr-qc/0508067].

[6] T. Damour, P. Jaranowski and G. Schaefer, Phys. Rev. D **77**, 064032 (2008) [arXiv:0711.1048 [gr-qc]].

[7] J. Steinhoff, S. Hergt and G. Schaefer, Phys. Rev. D **77**, 081501 (2008) [arXiv:0712.1716 [gr-qc]].

[8] R. V. Wagoner and C. M. Will, Astrophys. J. **210** (1976) 764 [Erratum-ibid. **215** (1977) 984].

[9] L. Blanchet, G. Faye, B. R. Iyer and S. Sinha, arXiv:0802.1249 [gr-qc].

[10] K. G. Arun, A. Buonanno, G. Faye and E. Ochsner, arXiv:0810.5336 [gr-qc].

[11] Numerical INJection Analysis (NINJA) Project Home Page, http://www.gravity.phy.syr.edu/dokuwiki/doku.php?id=ninja:home